Proceedings Paper:
Uddin, SZ and Talukder, MA orcid.org/0000-0002-2814-3658 (2017) Reduction of detection volume in total internal reflection fluorescence microscopy using graphene. In: Proceedings of 9th International Conference on Electrical and Computer Engineering (ICECE 2016). ICECE 2016, 20-22 Dec 2016, Dhaka, Bangladesh. IEEE , pp. 143-146. ISBN 9781509029631

https://doi.org/10.1109/ICECE.2016.7853876

Reduction of Detection Volume in Total Internal Reflection Fluorescence Microscopy Using Graphene

Shiekh Zia Uddin,[1] and Muhammad Anisuzzaman Talukder[1,*]
[1]Department of Electrical and Electronic Engineering, Bangladesh University of Engineering and Technology
Dhaka 1205, Bangladesh
*anis@eee.buet.ac.bd

***Abstract*—We show that it is possible to decrease the thickness of the detection volume of total internal reflection fluorescence microscopy (TIRFM) by ∼35% using a graphene layer in the interface between glass and water layers of a typical TIRFM structure without sacrificing the fluorescence intensity. The highly mobile surface bound electrons of a graphene mono-layer quenches the fluorophores that are less than ∼40 nm away from it. The decreased detection volume using the proposed structure will increase the resolution of a typical TIRFM technique. We find that the results are qualitatively similar for different incidence angles and polarizations of the excitation field. So, the proposed structure will also find applications in variants of TIRFM techniques, e.g., where incidence angles and polarizations are varied.**

***Index Terms*—Total Internal Reflection Fluorescence Microscopy, Graphene, and Detection Volume.**

I. Introduction

When light propagating through a medium of high index of refraction (glass) encounters a planar interface with a medium of lower index of refraction (water), it undergoes total internal reflection for incidence angles greater than the critical angle. Although totally reflected, the incident beam creates an evanescent electromagnetic field that penetrates into the medium of low index of refraction and decays exponentially from the interface [1]. Total internal reflection fluorescence microscopy (TIRFM) employs this evanescent field to selectively excite fluorophores only in a very thin layer near the substrate, thereby achieving resolution much greater than that possible by the diffraction limited optics [2], [3]. TIRFM has been used for the last three decades in a wide range of applications, e.g., to image single molecules attached to planar surfaces and to study the position, orientation and dynamics of molecules, and organelles in living culture cells near the contact regions with the glass [4], [5], [6].

Graphene is a single atomic layer of carbon arranged in a hexagonal lattice [7], which has drawn intense interest after being first discovered in 2004 [8], [9]. Graphene has excellent mechanical strength, chemical stability, electro-optical tunability as well as the highest mobility of carriers (both electrons and holes) due to the unique conical band structure. Although, initially, graphene was widely explored for applications in electronics [10], in recent years, it has also shown promises as a key element in photonics [11], optoelectronics [12], plasmonics [13], metamaterials [14], and biology [15].

In this work, we propose a graphene-based TIRFM technique that will decrease the detection volume significantly and thus, will increase the resolution of microscopy significantly. In particular, we propose to place a graphene mono-layer in the interface between glass and water layers of a typical TIRFM technique. The mobile electrons of the graphene quench the fluorescence of the molecules that are very close to the graphene layer. This quenching effectively decreases the thickness of the detection volume ∼35% of that of a typical TIRFM technique without decreasing fluorescence intensity. The decreased detection volume will increase the resolution of TIRFM furthering the study of biology. We find that the detection volume decreases for all angles of incidence greater than the critical angle and polarizations of excitation field. So, the proposed structure can also be used to reduce detection volume in modified versions of TIRFM where incidence angle and polarization variations are used to acquire image, e.g., in polarized TIRFM.

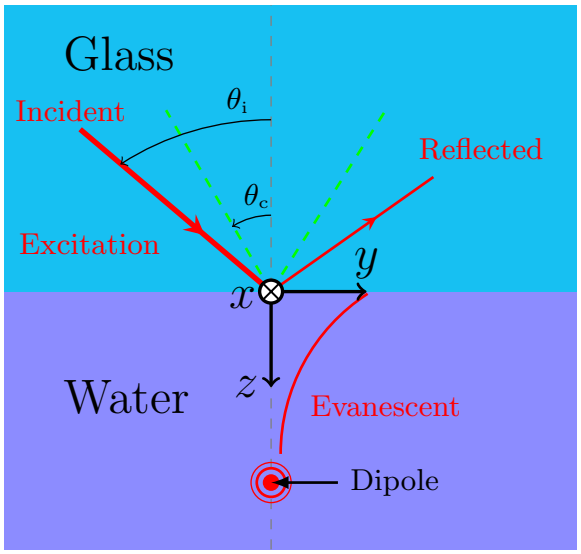

Fig. 1. Typical TIRFM structure where a glass-water interface is used to generate the evanescent excitation wave.

II. Proposed Structure

In Fig. 1, we show a schematic illustration of a typical structure that is used in TIRFM. The planar interface between a glass prism (dielectric constant $\epsilon_p = 2.304$) and water ($\epsilon_w = 1.769$) is used to generate the evanescent field. The sample labelled with fluorophores is placed in water near the interface. Excitation light incident from the prism side creates an exponentially decaying field profile in water from the interface. When fluorophores are excited by this evanescent light,

they become fluorescent and emit light, which is collected in the prism side and converted to microscopy image using appropriate optics [4]. In this work, we propose to place a graphene mono-layer in the glass-water interface of a typical structure. The excitation and collection schemes used in a typical TIRFM technique can also be used in the proposed technique.

III. Theoretical Background

A. The Optical Properties of Graphene Sheets

The widely used model for optical response of graphene is a very thin, two-sided surface characterized by a surface conductivity $\sigma(\omega, \mu_c, \Gamma, T)$, where ω is the angular frequency, μ_c is the chemical potential, Γ is the phenomenological scattering rate, and T is the temperature. Graphene's complex conductivity can be determined from the Kubo formula [16], [17], [18]

$$\sigma(\omega, \mu_c, \Gamma, T) = \sigma_{\text{intra}}(\omega, \mu_c, \Gamma, T) + \sigma_{\text{inter}}(\omega, \mu_c, \Gamma, T), \quad (1)$$

where σ_{intra} and σ_{inter} are intra-band and inter-band conductivity, respectively. The simplified intra-band contribution can be written as [18]

$$\sigma_{\text{intra}}(\omega, \mu_c, \Gamma, T) = i\frac{1}{\pi\hbar^2}\frac{e^2 k_B T}{(\omega + 2i\Gamma)} \left\{\frac{\mu_c}{k_B T} + 2\ln\left[\exp(-\frac{\mu_c}{k_B T}) + 1\right]\right\}, \quad (2)$$

and the inter-band contribution can be approximated as ($\mu_c >> k_B T$)

$$\sigma_{\text{inter}}(\omega, \mu_c, \Gamma, T) = i\frac{e^2}{4\pi\hbar}\ln\left[\frac{2|\mu_c| - \hbar(\omega + 2i\Gamma)}{2|\mu_c| - \hbar(\omega + 2i\Gamma)}\right], \quad (3)$$

where e is the electronic charge, $\hbar$ is the reduced Planck's constant, and k_B is the Boltzmann constant.

The chemical potential μ_c can be tuned by application of transverse gate voltage, electric field, magnetic field, and chemical doping. Typically chemical potential can be varied in the range of 0 to 1 eV. The phenomenological relaxation rate Γ can be approximated to be 0.1 meV, as reported in Ref. [19]. Because of the 2D nature of the graphene sheet, it behaves as a uni-axially anisotropic material, whose dielectric tensor can be written as

$$\overleftrightarrow{\epsilon}_{\text{gr}} = \begin{bmatrix} \epsilon_{g\parallel} & 0 & 0 \\ 0 & \epsilon_{g\parallel} & 0 \\ 0 & 0 & \epsilon_{g\perp} \end{bmatrix}, \quad (4)$$

where $\epsilon_{g\parallel}$ and $\epsilon_{g\perp}$ are the ordinary and extraordinary relative permittivities of graphene. Due to the two dimensional nature of graphene, the electric field that is polarized in the normal direction to the graphene layer cannot excite any current in it. So, the normal component of the permittivity or the extraordinary permittivity of graphene is given by $\epsilon_{g\perp} = 1$ [20]. The ordinary or the tangential permittivity can be defined by [17]

$$\epsilon_{g\parallel} = 1 + i\frac{\sigma(\omega, \mu_c, \Gamma, T)}{\omega\epsilon_0 t_{\text{gr}}}, \quad (5)$$

where $t_{\text{gr}} = 0.264$ nm is the thickness of a graphene mono-layer. The real and imaginary parts of the graphene tangential permittivity $\epsilon_{g\parallel}$ are shown in Figs. 2(a) and 2(b) for varying free-space wavelength (λ) and chemical potential (μ_c). We note that the resonance wavelength of the graphene blue-shifts as the chemical potential increases. In the analysis presented in this paper, we choose $\mu_c = 0.9$ meV.

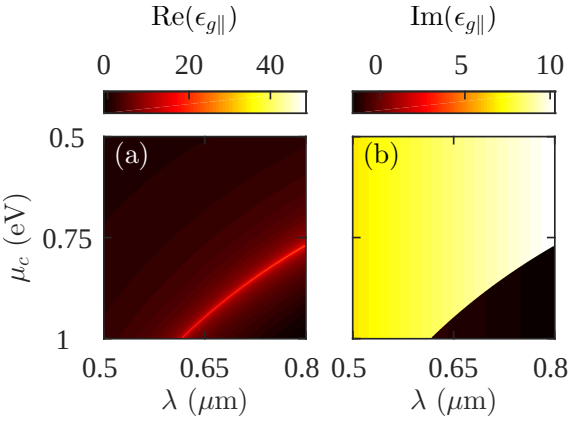

Fig. 2. (a) Real and (b) imaginary parts of the tangential permittivity of graphene ($\epsilon_{g\parallel}$) for varying wavelength (λ) and chemical potential (μ_c).

B. Total Internal Reflection

The critical angle for incident beam from glass is $\theta_c = \sin^{-1}\left(\sqrt{\epsilon_w/\epsilon_p}\right)$, where ϵ_w and ϵ_p are the dielectric constants of water and glass prism, respectively. For any polarization, if the incidence angle (θ_i) of an incident wave of wavelength λ is greater than the critical angle, then the transmitted wave is exponentially decaying with the distance from the interface. For both typical and proposed structures, the p-polarized excitation field can be written as [25]

$$\mathbf{E_{ex}} = E_0 t_p(\hat{\mathbf{x}}\sqrt{\epsilon_p \sin^2\theta_i - \epsilon_w} + j\hat{\mathbf{z}}\sqrt{\epsilon_p}\sin\theta_i)\exp(-z/2d), \quad (6)$$

and the s-polarized excitation field can be written as

$$\mathbf{E_{ex}} = E_0 t_s \hat{\mathbf{y}}\exp(-z/2d), \quad (7)$$

where $d = (\lambda/4\pi)\sqrt{\epsilon_p \sin^2(\theta_i) - \epsilon_w}$ is the penetration depth, E_0 is the amplitude of incident light, and t_p and t_s are Fresnel transmission coefficients for p- and s-polarized light, respectively. The Fresnel coefficients of anisotropic layered media are calculated using the 4×4 transfer matrix method [21], [22], [23].

C. Fluorescence Near Planar Stratified Media

Flurophores are molecules that absorb light at a specific frequency and emit at a different frequency. The emitted fluorescence is collected by appropriate optics. If the fluorophores are randomly oriented and the concentration $C(z)$ is only z dependent, then the collected fluorescence intensity from a pixel in a planar microscope can be written as [24], [25]

$$\begin{aligned} F &= k\int dz\ C(z)[w^{\perp}(z)Q^{\perp}(z) + w^{\parallel}(z)Q^{\parallel}(z)] \\ &= k\int dz\ C(z)g(z), \end{aligned} \quad (8)$$

where k is a proportionality constant consisting of conversion factors, normalization and arithmetic constants, $w^{\perp,\parallel}(z)$ are the weighting terms, and $Q^{\perp,\parallel}(z)$ are the collection efficiencies for vertical and horizontal dipoles. The weighing function $g(z) = [w^{\perp}(z)Q^{\perp}(z) + w^{\parallel}(z)Q^{\parallel}(z)]$ acts as a mask on the concentration profile and selects the region of sample volume whose concentration contributes to the collected fluorescence

intensity. The shape of the weighing function $g(z)$ determines the thickness of detection volume. Calculation of $g(z)$ requires evaluation of collection efficiencies and weighing terms.

Collection efficiency is the ratio of fluorescent energy collected by the imaging system to the total emitted energy and it depends on the position, orientation and environment of the fluorophore. The theory for calculating collection efficiencies for fluorophores in any stratified media is outlined in Refs. 24 and 25. We use this theory to calculate the collection efficiencies for horizontal and vertical dipoles in typical and proposed structures and show them in Fig. 3. In the proposed structure, the collection efficiencies decrease significantly if the fluorophores are near the interface.

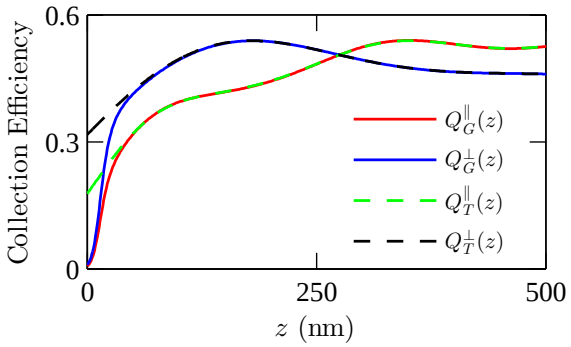

Fig. 3. Collection efficiency for horizontal and vertical dipoles in the proposed structure [$Q_G^{\parallel}(z)$ and $Q_G^{\perp}(z)$] and the typical structure [$Q_T^{\parallel}(z)$ and $Q_T^{\perp}(z)$], respectively.

If $\mathbf{E^{ex}} = \hat{\mathbf{x}}E_x^{ex} + \hat{\mathbf{y}}E_y^{ex} + \hat{\mathbf{z}}E_z^{ex}$ is the phasor representation of the excitation electric field, then the weighting terms can be written as

$$w^{\perp,\parallel}(z) = |E_x^{ex}|^2 w_x^{\perp,\parallel}(z) + |E_y^{ex}|^2 w_y^{\perp,\parallel}(z) + |E_z^{ex}|^2 w_z^{\perp,\parallel}(z). \quad (9)$$

The detail forms of the parameters $w_{x,y,z}^{\perp,\parallel}(z)$ are given in Ref. 24. The parameters $w_{x,y,z}^{\perp,\parallel}(z)$ are functions of lifetime ratio $\eta(z) = \tau^{\perp}(z)/\tau^{\parallel}(z)$, where $\tau^{\parallel}(z)$ and $\tau^{\perp}(z)$ are the lifetimes of horizontal and vertical dipoles situated at height z.

IV. Results

The lifetimes for horizontal and vertical dipoles in the typical and proposed structures are shown in Fig. 4(a). The lifetime ratio function $\eta(z)$ for the typical and proposed structures is shown in Fig. 4(b). We note a difference in $\eta(z)$ in a typical and the proposed structure when the fluorophores are near the interface. The weighing terms, which are functions of the lifetime ratio $\eta(z)$ are shown in Fig. 4(c).

Figure 5 shows the weighing function $g(z)$ that selects a region of the sample, where the fluorophores are excited to emit light and contribute to the collected fluorescence. Figure 5(a) shows the weighing function for different values of incidence angle of p-polarized excitation field for the typical TIRFM structure. We note that, for any incidence angle, the weighing function decreases with height (z) from the glass-water interface. The weighing function in the proposed structure is shown in Fig. 5(b) for p-polarized excitation. We note that, for a region close to the interface, the weighing function is zero due to quenching of fluorophores by the graphene layer. The quenching of fluorescence decreases the

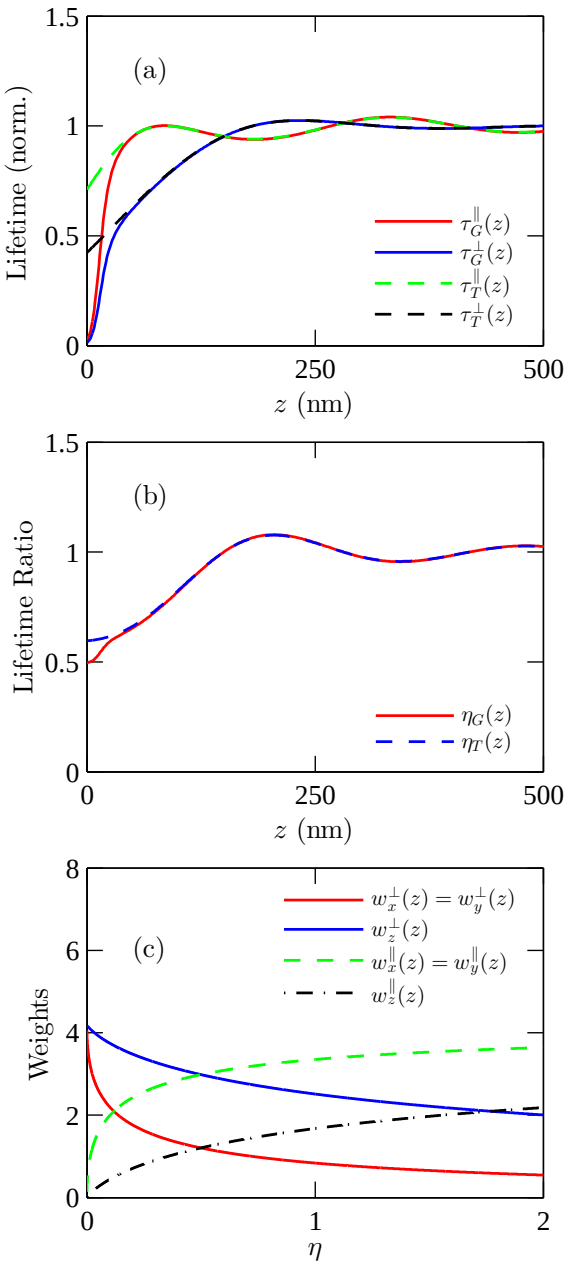

Fig. 4. (a) Lifetime of horizontal and vertical dipoles with position in typical and proposed structures, (b) Lifetime ratio with position in typical and proposed structures, and (c) weighing terms with lifetime ratio.

effective thickness of sample layer excited by the p-polarized field. We observe similar results when the excitation light is s-polarized, as shown in Figs. 5(c) and 5(d). The amplitude level of the weighing functions in the typical and proposed structures are similar.

We calculate the full width at the half maximum (FWHM) of the weighing function $g(z)$ to determine the thickness of the detection volume in the z-direction. Figure 6(a) shows the FWHM thickness of the detection volume for p-polarized excitation in the typical (δ_T^p) and the proposed structures (δ_G^p). We find that the FWHM thickness of $g(z)$ of the proposed structure decreases by $\sim$80 nm and $\sim$40 nm for an angle of incidence of 65° and 85°, respectively. Similar quantitative results are found for s-polarized excitation.

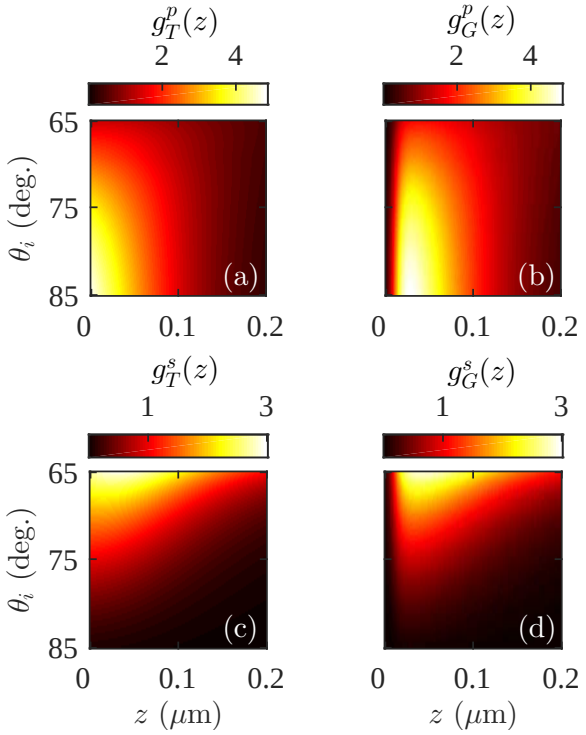

Fig. 5. Weighing function $g(z)$ for varying incidence angle and position in the (a) typical and (b) proposed structure for p-polarized light and (c) typical and (b) proposed structure for s-polarized light.

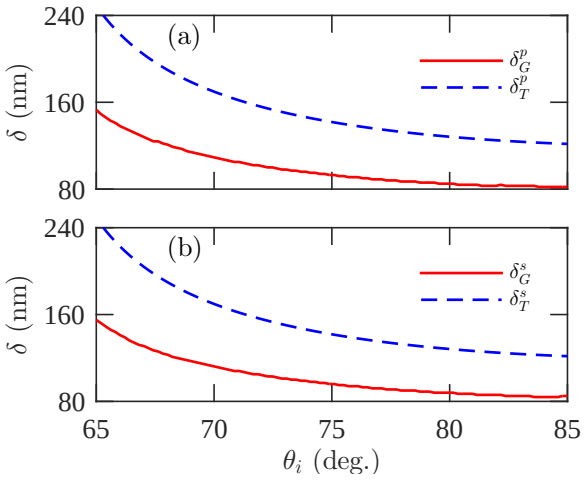

Fig. 6. Detection volume thickness for (a) p- and, (b) s-polarized light in the typical and proposed TIRFM structure.

V. Conclusion

We used mono-layer graphene in the glass-water interface to modify the behaviour of TIRFM and found decreased detection volume without decreasing fluorescence intensity. We found that the detection volume in TIRFM can decrease as much as ∼35% with the use of a graphene mono-layer. The results remain qualitatively the same for both p- and s-polarized light.

VI. Acknowledgement

We gratefully acknowledge the support received from the Department of Electrical and Electronic Engineering of Bangladesh University of Engineering and Technology (BUET) in carrying out this work.

References

[1] S. J. Orfanidis, *Electromagnetic waves and antennas*, Rutgers University, New Brunswick, NJ, 2002.
[2] D. Axelrod, "Total internal reflection fluorescence microscopy," *Methods in Cell Biology*, vol. 30, pp. 245–270, 1989.
[3] D. Axelrod, E. H. Hellen, and R. M. Fulbright, *Topics in fluorescence spectroscopy*, Springer, 2002.
[4] A. L. Mattheyses, S. M. Simon, and J. Z. Rappoport, "Imaging with total internal reflection fluorescence microscopy for the cell biologist," *Journal of Cell Science*, vol. 123, pp. 3621–3628, 2010.
[5] D. S. Johnson, J. K. Jaiswal, and S. Simon, "Total internal reflection fluorescence (TIRF) microscopy illuminator for improved imaging of cell surface events," *Current Protocols in Cytometry*, vol. 61, pp. 12–29, 2012.
[6] D. Axelrod, "Total internal reflection fluorescence microscopy in cell biology," *Traffic*, vol. 2, pp. 764–774, 2001.
[7] A. C. Neto, F. Guinea, N. Peres, K. S. Novoselov, and A. K. Geim, "The electronic properties of graphene," *Reviews of Modern Physics*, vol. 81, pp. 109, 2009.
[8] K. S. Novoselov, A. K. Geim, S. Morozov, D. Jiang, Y. Zhang, S. Dubonos, , I. Grigorieva, and A. Firsov, "Electric field effect in atomically thin carbon films," *Science*, vol. 306, pp. 666–669, 2004.
[9] K. Novoselov, A. K. Geim, S. Morozov, D. Jiang, M. Katsnelson, I. Grigorieva, S. Dubonos, and A. Firsov, "Two-dimensional gas of massless dirac fermions in graphene," *Nature*, vol. 438, pp. 197–200, 2005.
[10] A. K. Geim, K. Novoselov, and S. Konstantin, "The rise of graphene," *Nature Materials*, vol. 6, pp. 183–191, 2007.
[11] F. Bonaccorso, Z. Sun, T. Hasan, and A. Ferrari, "Graphene photonics and optoelectronics," *Nature Photonics*, vol. 4, pp. 611–622, 2010.
[12] C.-H. Liu, Y.-C. Chang, T. B. Norris, and Z. Zhong, "Graphene photodetectors with ultra-broadband and high responsivity at room temperature," *Nature Nanotechnology*, vol. 9, pp. 273–278, 2014.
[13] A. Grigorenko, M. Polini, and K. Novoselov, "Graphene plasmonics," *Nature Photonics*, vol. 6, pp. 749–758, 2012.
[14] M. A. Othman, C. Guclu, and F. Capolino, "Graphene-based tunable hyperbolic metamaterials and enhanced near-field absorption," *Optics Express*, vol. 21, pp. 7614–7632, 2013.
[15] K. Kostarelos and K. S. Novoselov, "Exploring the interface of graphene and biology," *Science*, vol. 344, pp. 261–263, 2014.
[16] L. Falkovsky and S. Pershoguba, "Optical far-infrared properties of a graphene monolayer and multilayer," *Physical Review B*, vol. 76, pp. 153410, 2007.
[17] L. Falkovsky, "Optical properties of graphene," *Journal of Physics: Conference Series*, vol. 129, pp. 012004, 2008.
[18] G. W. Hanson, "Dyadic greens functions and guided surface waves for a surface conductivity model of graphene," *Journal of Applied Physics*, vol. 103, pp. 064302, 2008.
[19] A. Vakil and N. Engheta, "Transformation optics using graphene," *Science*, vol. 332, pp. 1291–1294, 2011.
[20] B. Zhu, G. Ren, S. Zheng, Z. Lin, and S. Jian, "Nanoscale dielectric-graphene-dielectric tunable infrared waveguide with ultrahigh refractive indices," *Optics Express*, vol. 21, pp. 17089–17096, 2013.
[21] D. W. Berreman, "Optics in stratified and anisotropic media: 4×4-matrix formulation," *Journal of the Optical Society of America*, vol. 62, pp. 502–510, 1972.
[22] P. Yeh,"Optics of anisotropic layered media: a new 4×4 matrix algebra," *Surface Science*, vol. 96, pp. 41–53, 1980.
[23] M. Schubert, "Polarization-dependent optical parameters of arbitrarily anisotropic homogeneous layered systems," *Physical Review B*, vol. 53, pp. 4265, 1996.
[24] E. H. Hellen and D. Axelrod, "Fluorescence emission at dielectric and metal-film interfaces," Journal of the Optical Society of America B," vol. 4, pp. 337–350, 1987.
[25] L. Novotny and B. Hecht, *Principles of nano-optics*, Cambridge university press, 2012.